Inorg. Chem. **2003**, *42*, 8773–8782

Inorganic Chemistry Article

Reaction of Bare VO^+ and FeO^+ with Ammonia: A Theoretical Point of View

Sandro Chiodo, Olga Kondakova, Maria del Carmen Michelini, Nino Russo,* and Emilia Sicilia

Dipartimento di Chimica and Centro di Calcolo ad Alte Prestazioni per Elaborazioni Parallele e Distribuite-Centro d'Eccellenza MURST, Università della Calabria, I-87030 Arcavacata di Rende, Italy

Received July 22, 2003

The potential energy surfaces corresponding to the dehydration reaction of NH_3 by VO^+ ($^3\Sigma$, $^1\Delta$, $^5\Sigma$) and FeO^+ ($^6\Sigma$, $^4\Delta$) metal oxide cations have been investigated within the framework of the density functional theory in its B3LYP formulation and by employing new optimized basis sets for iron and vanadium. The reaction is proposed to occur through two hydrogen shifts from the nitrogen to the oxygen atom giving rise to multicentered transition states. Possible spin crossing between surfaces at different spin multiplicities has been considered. The energy profiles are compared with the corresponding ones for the insertion of bare cations to investigate the influence on reactivity of the presence of the oxygen ligand. The topological analysis of the gradient field of the electron localization function has been used to characterize the nature of the bonds for all the minima and transition states along the paths.

1. Introduction

The gas-phase chemistry of transition metal ions has been widely studied and developed in the last two decades due to the crucial role that these species play in various areas of chemical research as organic chemistry, biochemistry, and, most importantly, catalytic processes. Early studies mainly concern the reactivity of bare metal ions[1−11] and have revealed their very high reactivity toward small molecules containing prototypical bonds, depending on the nature of metal. Gas-phase studies are attractive tools for the examinations of this kind of systems, both experimentally and theoretically, since any contribution deriving from the presence of solvent counterions and ligands can be rigorously excluded. In the same way, the gas-phase environment offers the possibility to study the effects of a single ligand and, by sequentially adding ligands to the metal ion, allows us to analyze its influence to the reactivity. Consequently, during the last 10 years a growing number of papers has appeared devoted to the study of gas-phase reactivity of metals bearing one or several ligands, enhancing reactivity as a function of the nature of the ligands.[6,12−23]

* To whom correspondence should be addressed. E-mail: nrusso@unical.it.

(1) Allison, J.; Freas, R. B.; Ridge, D. P. *J. Am. Chem. Soc*. **1979**, *101*, 1332.
(2) *Gas-Phase Inorganic Chemistry*; Russel, D. H., Ed., Plenum: New York, 1989; p 412.
(3) Armentrout, P. B.; Beauchamp, J. L. *Acc. Chem. Res.* **1993**, *26*, 213.
(4) Armentrout, P. B. In *Selective Hydrocarbons Activation: Principles and Progress*; Davies, J. A., Watson, P. L., Greenberg, A., Liebman, J. F., Eds.; VCH: New York, 1990.
(5) Armentrout, P. B. *Annu. Rev. Phys. Chem*. **1990**, *41*, 313.
(6) Eller, K.; Schwarz, H. *Chem. Rev.* **1991**, 9*1*, 1121.
(7) (a) Weisshaar, J. C. *Adv. Chem. Phys.* **1992**, 8*2*, 213. (b) Weisshaar, J. C. *Acc. Chem. Res.* **1993**, *26*, 213.
(8) Armentrout, P. B.; Kickel, B. L. In *Organometallic Ion Chemistry*; Freiser, B. S., Ed.; Kluwer: Dordrecht, The Netherlands, 1996.
(9) Armentrout, P. B. In *Topics in Organometallic Chemistry*; Brown, J. M., Hofmann, P., Eds.; Springer-Verlag: Berlin, 1999.
(10) Crabtree, R. H. *The Organometallic Chemistry of the Transition Metals*, 2nd ed.; John Wiley & Sons: New York, 1994.
(11) Somorjai, G. A. *Introduction to Surface Chemistry and Catalysis*; John Wiley & Sons: New York, 1994.
(12) Jacobson, D. B.; Freiser, B. S. J. *Am. Chem. Soc.* **1984**, *106*, 3891.
(13) Jackson, T. C.; Jacobson, D. B.; Freiser, B. S. *J. Am. Chem. Soc*. **1984**, *106*, 1252.
(14) Huang, S. K.; Allison, J. *Organometallics* **1983**, *2*, 833.
(15) Freas, R. B.; Ridge, D. P. *J. Am. Chem. Soc.* **1980**, *102*, 7129.
(16) Fiedler, A.; Schröder, D.; Shaik, S.; Schwarz, H. *J. Am. Chem. Soc.* **1994**, *116*, 10734.
(17) Ryan, M. F.; Fiedler, A.; Schroder, D.; Schwarz, H. *Organometallics* **1994**, *13*, 4072.
(18) Clemmer, D. E.; Aristov, N.; Armentrout, P. B. *J. Phys. Chem.* **1993**, *97*, 544.
(19) Clemmer, D. E.; Chen, Y.-M.; Khan, F. A.; Armentrout, P. B. *J. Phys. Chem.* **1994**, *98*, 6522.
(20) Chen, Y.-M.; Clemmer, D. E.; Armentrout, P. B. *J. Am. Chem. Soc.* **1994**, *116*, 7815.
(21) Bushnell, J. E.; Kemper, P. R.; Maitre, P.; Bowers, M. T. *J. Am. Chem. Soc.* **1994**, *116*, 9710.
(22) van Koppen, P. A. M.; Kemper, P. R.; Bushnell, J. E.; Bowers, M. T. *J. Am. Chem. Soc.* **1995**, *117*, 2098.

10.1021/ic0348650 CCC: $25.00

Published on Web 11/20/2003

We have yet studied[24−27] the state-specific chemistry of first-row transition metal bare cations with water, ammonia, and methane, particularly of V^+ in its $^5D(3d^4)$ ground and $^3F(3s^14d^3)$ excited electronic states[24] and Fe^+ in its $^6D(4s^13d^6)$ ground and $^4F(3d^7)$ excited electronic states.[27] In this paper, we report the results of a study of the insertion reaction of gas-phase diatomic VO^+ and FeO^+ metal oxides into the N−H bond of ammonia. The focus of this study involving metal oxides is to assess their ability to activate simple bonds and compare their reactivity patterns with those of the corresponding bare cations to determine the differences in behavior induced by the addition of the oxygen ligand. Due to the importance that two-state reactivity (TSR) has in affecting reaction mechanisms of organometallic transformations,[28,29] the influence of possible crossings between high- and low-spin surfaces has also been examined.

When first row transition metal cations insert into X−H (X = O, N, C) bonds, the H_2 elimination process is the most thermodynamically favored for early and middle metals. Activation of the same bonds by transition metal oxides, on the contrary, very often does not give dehydrogenation products, and the H_2O elimination process preferentially occurs only for the ammonia molecule. The investigation of the reactivity of oxides toward ammonia, therefore, allows a direct comparison between bare transition metal cations, active in dehydrogenation, and their oxides. However, the work on this subject is really scarce, and to our knowledge, only a few experimental data concerning VO^+ and FeO^+ oxides interacting with ammonia exist in the literature. The reaction of FeO^+ with NH_3 has been investigated by Fourier transform ion cyclotron resonance mass spectrometry[30] and discussed in a paper on the oxidative addition of the N−H bond in NH_3.[31] In the same paper, some indications are reported regarding the reaction of ammonia with vanadium oxide. Recall, nevertheless, that in 1996, Gehret and Irion performed preliminary studies on the reactivity of the $Fe_2O_2^+$ cation with ammonia.[32]

The mechanism experimentally proposed involves formation of MNH^+ and MOH^+ as ionic products:

$$MO^+ + NH_3 \rightarrow MNH^+ + H_2O$$

$$MO^+ + NH_3 \rightarrow MOH^+ + NH_2$$

To analyze the proposed mechanism, the electronic and molecular structures of the various compounds implicated in the insertion reactions of VO^+ and FeO^+ into the N−H bond of ammonia, as well as the corresponding reaction paths, have been determined by using the density functional theory (DFT). It is well-known that DFT fails in the description of atomic ground states, probably because of a bias toward $3d^n$ over $3d^{n-1}4s^1$ configurations, and it is unclear how this error influences molecular calculations. Therefore, newly developed basis sets[33] for iron and vanadium, optimized for the B3LYP functional, have been employed to calculate DFT reaction pathways.

2. Method

Geometry optimizations as well as frequency calculations for all the stationary points considered here have been performed at the density functional level of theory, employing the hybrid B3LYP[34,35] functional. Previous investigations on transition metal compounds have indicated, without any doubt, that the performance of the B3LYP DF in predicting numerous properties such as binding energies, geometries, frequencies, and so on is very satisfactory. Moreover, although the accuracy of the results is comparable to that obtainable by highly correlated ab initio methods, less demanding computational efforts are required.[36−42] However, one of the shortcomings of the density functional approaches is the incorrect prediction of the ordering of ground and excited electronic states of atoms. This trend should persist in the molecular calculations, although it is not clear in which way this error translates quantitatively. Therefore, completely newly developed basis sets[33] for iron and vanadium atoms, optimized ad hoc, have been employed to localize minima and transition states relevant for the examined processes and to build up the corresponding potential energy surfaces. These basis sets have been optimized by us for all the 3d transition metal elements starting from the corresponding DZVP ones[43] optimizing variationally the linear combination coefficients, which define a contracted function.[44] In comparison to the traditional DZVP basis sets,[43] optimized for local functionals, the new ones improve the description of the ground and low lying excited energy levels of first-row transition metal atoms and cations.[27,45] Therefore, we are confident that the limits in a quantitatively reliable description at the B3LYP/DZVP level of the features of the studied PES's can be overcome by using these new B3LYP-optimized basis sets. For the other elements, the traditional TZVP basis sets have been employed, and we will refer to this level of computation as B3LYP/DZVP$_{opt}$, emphasizing the role of the basis sets used for the metals. For each optimized

(23) Tjelta, B. L.; Armentrout, P. B. *J. Am. Chem. Soc.* **1995**, *117*, 5531.
(24) Russo, N.; Sicilia, E. *J. Am. Chem. Soc*. **2001**, *123*, 2588.
(25) Russo, N.; Sicilia, D. *J. Am. Chem. Soc*. **2002**, *124*, 1471.
(26) Michelini, M. C.; Russo, N.; Sicilia, E. *J. Phys. Chem*. **2002**, *106*, 8937.
(27) Chiodo, S.; Kondakova, O.; Irigoras, A.; Michelini, M. C.; Russo, N.; Sicilia, E.; Ugalde, J. M. *J. Phys. Chem*., submitted.
(28) Armentrout, P. B. *Science* **1991**, *251*, 175.
(29) Schröder, D.; Shaik, S.; Schwarz, H. *Acc. Chem. Res*. **2000**, *33*, 139.
(30) Brönstrup, M.; Schröder, D.; Schwarz, H. *Chem. Eur. J*. **1999**, *5*, 1176.
(31) Buckner, S. W.; Gord, J. R.; Freiser, B. S. *J. Am. Chem. Soc*. **1988**, *110*, 6606.
(32) Gehret, O.; Irion, M. P. *Eur. J. Chem*. **1996**, *2*, 598.
(33) Chiodo, S.; Russo, N.; Sicilia, E. *J. Comput. Chem.*, submitted.
(34) Becke, A. D. *J. Chem. Phys.* **1993**, *98*, 5648.
(35) Lee, C.; Yang, W.; Parr, R. G. *Phys. Rev. B* **1988**, *37*, 785.
(36) Aschi, M.; Bronstrup, M.; Diefenbach, M.; Harvey, J. N.; Schröder, D.; Schwarz, H. *Angew. Chem., Int. Ed.* **1998**, *37*, 829.
(37) Ricca, A.; Bauschlicher, C. W., Jr. *Chem. Phys. Lett*. **1995**, *245*, 150.
(38) Holthausen, M. C.; Fiedler, A.; Schwarz, H.; Koch, W. *J. Phys. Chem*. **1996**, *100*, 6236.
(39) Bauschlicher, C. W., Jr.; Ricca, A.; Partridge, H.; Langghoff, S. R. In *Recent Advances in Density Functional Theory, Part II*; Chong, D. P., Ed.; World Scientific Publishing Co.: Singapore, 1997. See also references therein.
(40) Sodupe, M.; Branchadell, V.; Rosi, M.; Bauschlicher, C. W., Jr. *J. Phys. Chem*. **1997**, *101*, 7854.
(41) Pavlov, M.; Siegbahn, P. E. M.; Sandström, M. *J. Phys. Chem. A* **1998**, *102*, 219.
(42) Yi, S. S.; Blomberg, M. R. A.; Siegbahn, P. E. M.; Weisshaar, M. *J. Phys. Chem*. **1998**, *102*, 395.
(43) Goudbout, N.; Salahub, D. R.; Andzelm, J.; Wimmer, E. *Can. J. Chem*. **1992**, *70*, 560.
(44) Gianolio, L.; Pavani, R.; Clementi, E. *Gazz.Chim. Ital.* **1978**, *108*, 181.
(45) Calaminici, P.; Köster, A. M.; Carrington Jr., T.; Roy, P. N.; Russo, N.; Salahub, D. R. *J. Chem. Phys.* **2001** *114*, 4036.

stationary point, vibrational analysis was performed to determine its character (minimum or saddle point) and to evaluate the zero-point vibrational energy (ZPVE) corrections, which are included in all relative energies.

All the calculations reported here have been carried out with the GAUSSIAN94/DFT[46] code.

We have analyzed the nature of the interactions present in all the species involved in the potential energy surfaces by means of a topological description of them. In particular, we have used the topological analysis of the gradient vector field of the Becke and Edgecombe[47] electron localization function (ELF) as implemented by Silvi and co-workers.[48,49] The ELF, η(r), can be interpreted as a measure of the electron localization in atomic and molecular systems, i.e., as the conditional probability of finding two electrons with the same spin around a reference point.[48] The analysis of the ELF gradient field provides a mathematical model enabling the partition of the molecular position space in basins of attractors, which present in principle a one to one correspondence with chemical local objects such as bonds and lone pairs. These basins are either core basins, usually labeled C(A), or valence basins, V(A,...), belonging to the outermost shell and characterized by the number of core basins with which it shares a common boundary, which is called the synaptic order. In this representation, the monosynaptic basins correspond to the nonbonded pairs of the usual Lewis representation whereas the di- and polysynaptic basins are related to bonds.

To analyze the evolution of the bonding during the reaction, we used of the so-called bond evolution theory,[50] within the framework of Thom's catastrophe theory.[51] From this viewpoint, a chemical reaction is considered as a series of topological changes occurring along the reaction path. The parameters defining the reaction pathway, such as the nuclear coordinates and the electronic states, constitute the control space. There are two important indicators in using this methodology, i.e., the number of basins, which is called the morphic number (μ), and the before-mentioned synaptic order of basins. The evolution of the bonding along the reaction path is modelled by the changes observed in the morphic number ($\Delta\mu$). According to the variation of this number between products and reactants, three types of reactions are possible, namely, plyomorphic ($\Delta\mu > 0$), tautomorphic ($\Delta\mu = 0$), and miomorphic ($\Delta\mu < 0$). Tautomorphic processes are either isosynaptic if the basin synaptic order is not changed or diffeosynaptic otherwise (see ref 49 for a detailed discussion). Each structure is only possible for values of the control parameters belonging to definite ranges called structural stability domains. For any two points of the control space belonging to a given structural stability domain, there is the same number of critical points of each type in the ELF gradient field. This technique shows how the bonds are formed and broken and also emphasizes the importance of the geometrical constraints in a chemical reaction. Moreover, the identification of the elementary catastrophe and, therefore, the knowledge of its universal unfolding yields the dimension of the active control space governing the reaction.[50,51] From a quantitative viewpoint, the evolution of the total and spin basin populations along the path provides keys to understanding the role played by the different chemical interactions.

In previous work,[27,52] we have used this methodology to analyze the evolution of the chemical bonds finding that this method constitutes a reliable tool to study this class of reactions.

ELF calculations have been carried out with the TopMod package developed at the Laboratoire de Chimie Théorique de l'Université Pierre et Marie Curie.[53,54] Isosurfaces have been visualized with the public domain scientific visualization and animation program for high performance graphic workstations named Scian.[55]

3. Results and Discussion

The reaction for dehydrogenation of ammonia by MO^+ to give water is proposed to occur in a two step concerted manner through oxidative addition of NH_3 across the M−O bond to form the hydroxy intermediate, $HO-M^+-NH_2$, which corresponds to the $H-M^+-NH_2$ intermediate along the analogous surfaces for the insertion of the bare cations. The reaction pathway involves formation in the first step of a stable ion−dipole complex. In this adduct, one H−N bond is activated, and the insertion is realized through a transition state corresponding to a hydrogen shift from the nitrogen to the oxygen atom. Electron pairing of the valence electrons of the metal to form two covalent O−M and M−N bonds leads to the insertion intermediate, $HO-M^+-NH$, of low-spin multiplicity. If the ground state of the reacting species is a high one, the spin is not conserved along the path and a surface crossing is likely to occur. After this step, a second hydrogen migration from nitrogen to oxygen, corresponding to a four-center transition state, yields the intermediate H_2O-M^+-NH, from which the reaction can proceed toward dehydration products through a simple cleavage of the M−O bond. The side product MOH^+ can be formed by direct breaking of the metal−nitrogen bond from the hydroxy intermediate.

In the following sections, the details of the PES's corresponding to the interaction of vanadium and iron cationic oxides with ammonia, for both the ground and the low-lying excited states, will be examined. With the purpose of extracting useful information on the bonding and its evolution along the paths, the results of the ELF topological analysis are reported for the most significant minima and transition states.

VO^+ Insertion into N−H Bond. B3LYP/DZVP$_{opt}$ geometrical parameters of stationary points for the lowest energy triplet spin state are reported in Figure 1, while the corresponding potential energy profiles are depicted in Figure 2.

(46) Frisch, M. J.; Trucks, G. W.; Schlegel, H. B.; Gill, P. M. W.; Johnson, B. G.; Robb, M. A.; Cheeseman, J. R.; Keith, T.; Petersson, G. A.; Montgomery, J. A.; Raghavachari, K.; Al-Laham, M. A.; Zakrzewski, V. G.; Ortiz, J. V.; Foresman, J. B.; Cioslowski, J.; Stefanov, B. B.; Nanayakkara, A.; Challacombe, M.; Peng, C. Y.; Ayala, P. Y.; Chen, W.; Wong, M. W.; Andres, J. L.; Replogle, E. S.; Gomperts, R.; Martin, R. L.; Fox, D. J.; Binkley, J. S.; Defrees, D. J.; Baker, J.; Stewart, J. P.; Head-Gordon, M.; Gonzalez, C.; Pople, J. A. *Gaussian 94*, revision A.1; Gaussian, Inc.: Pittsburgh, PA, 1995.
(47) Becke, A. D.; Edgecombe, K. E. *J. Chem. Phys.* **1990**, *92*, 5397.
(48) Silvi, B.; Savin, A. *Nature* **1994**, *371*, 683.
(49) Noury, S.; Colonna, F.; Savin, A.; Silvi, B. *J. Mol. Struct.* **1998**, *450*, 59.
(50) Krokidis, X.; Noury, S.; Silvi, B. *J. Phys. Chem. A* **1997**, *101*, 7277.
(51) Thom, R. *Stabilitè Structurelle et Morphogénese*; Interditions: Paris, 1972.
(52) Michelini, M. C.; Sicilia, E.; Russo, N.; Alikhani, E.; Silvi, B. *J. Phys. Chem. A* **2003**, *107*, 4862.
(53) Noury, S.; Krokidis, X.; Fuster, F.; Silvi, B. *TopMod Package*; l'Université Pierre et Marie Curie: Paris, 1997.
(54) Noury, S.; Krokidis, X.; Fuster, F.; Silvi, B. *Comput. Chem.* **1999**, *23*, 597.
(55) Pepke, E.; Muray, J.; Lyons, J. *Scian (Supercomputer Computations Res. Inst.)*; Florida State University: Tallahassee, FL, 1993.

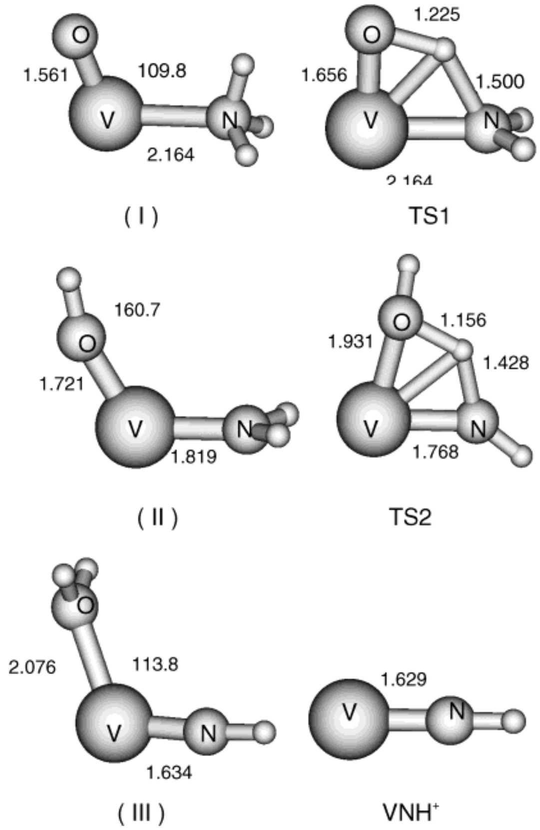

Figure 1. Geometric parameters of minima and transition states on the B3LYP/DZVP$_{opt}$ triplet potential energy surface for the reaction of VO^+ with NH_3. Bond lengths are in angstroms and angles in degrees.

The VO^+ cation has a triplet ground state ($^3\Sigma$) separated by 24.5 kcal/mol from the closest singlet ($^1\Delta$) excited electronic state. The next quintet ($^5\Sigma$) excited state lies 79.35 kcal/mol above the ground state. This computed value is in the range (76.1−96.9 kcal/mol) of the proposed experimental values,[56] being closer to the lower limit. We have investigated the paths corresponding to these three multiplicities, but the most stable triplet state of the oxide cation corresponds also to the most stable state of the products and no crossing is observed to occur during the course of the reaction. Along the triplet path, the first step of the reaction is the exothermic formation of the ion−molecule complex (I), which is stabilized with respect to the separated building blocks by 52.6 kcal/mol. The next step of the reaction is the insertion of VO^+ into the N−H bond of ammonia through the formation of a transition state TS1, which corresponds to the migration of a hydrogen atom from nitrogen to the oxygen atom. The insertion intermediate (II) is more stable than the dissociation limit by 22.3 kcal/mol, and from it, the reaction proceeds to yield the molecular water complex $(H_2O)V^+$−NH (III) after passing through the TS2 four-center transition state. Although both the activation barriers that are necessary to surmount to obtain the final complex are very high, it is worth noting that the first barrier is below the ground state reactants limit and the second one is only 6.4 kcal/mol above. The dehydration products, finally, are formed directly from (III) without an energy barrier, with a predicted endothermicity of 15.6 kcal/mol.

The VOH^+ product is obtained directly by breaking of the V−N bond in the intermediate (II) and is 19.9 kcal/mol higher in energy with respect to the asymptote.

Now we will summarize the results of the topological analysis of the electron localization function for all the minima and transition states corresponding to the lowest-energy triplet PES. Figure 3 shows the localization domains (i.e., the volumes bounded by a given isosurface) corresponding to these structures. Table 1 collects quantitative information drawn from ELF analysis, specifically, the electron basin populations ($\bar{N}$), and basin integrated spin densities ($\langle S_Z \rangle$) corresponding to the most relevant basins.

The first ion−molecule complex is characterized by the presence of nine basins, four of which can be classified as disynaptic ones, namely, the three V(N,H) basins corresponding to the three N−H bonds of NH_3, and a V(V,O) dysinaptic basin, that accounts for the V−O covalent bond. No disynaptic basin is formed between the metal and the NH_3 molecule. Instead, a monosynaptic V(N) basin that accounts for the nitrogen lone pair, with a population of 2.04 electrons, is present. The basin populations and their spatial distributions allow us to classify the interaction between the metal oxide and the NH_3 molecule as electrostatic in nature. Indeed, the basin populations of the VO^+ fragment are very close to the ones corresponding to the VO^+ (^{3}S) ground state, as can be seen in Table 1. Our ELF analysis of the first-complex VO^+ fragment completely agrees with the previously reported one.[57,58]

Following the reaction path to the first transition state, TS1, important topological changes take place. A fold bifurcation catastrophe[50] breaks the N−H covalent bond giving rise to the formation of two monosynaptic basins, V(H) and V(N), which are populated by 0.53 and 1.50 electrons, respectively. Electron charge is transferred from the vanishing basin to the disynaptic V(V,N) basin, which is formed in this step of the reaction, and has a population of 2.06 electrons. The atomic contributions to this basin, with more than 90% of the population coming from the nitrogen, indicates that the V−N bond can be seen as a "donor−acceptor" one.

In going from I to TS1, the population of the V(O) basin increases by about 0.5 electrons, whereas the V(N) monosynaptic basin suffers a loss of charge of almost the same amount, producing a charge transfer to the V(V,N) basin, which is formed in this step of the reaction. The electronic population of the V−O bond is redistributed in a more symmetrical way, being split between two V(V,O) disynaptic basins. As has been previously underlined,[49] the number of basins of a given type is ruled more by symmetry that by perfect pair formation. It is clear that in this intermediate

(56) Dyke, J. M.; Gravenor, B. W. J.; Hastings, M. P.; Morris, A. *J. Phys. Chem. A* **1985**, *89*, 4613.

(57) Calatalyud, M.; Silvi, B.; Andrés, J.; Beltran, A. *Chem. Phys. Lett.* **2001**, *333*, 493.

(58) Calatalyud, M.; Berski, S.; Beltran, A.; Andrés, J. *Theor. Chem. Acc.* **2002**, *108*, 12.

(59) Krokidis, X.; Silvi, B.; Alikhani, M. E. *Chem. Phys. Lett.* **1998**, *292*, 35.

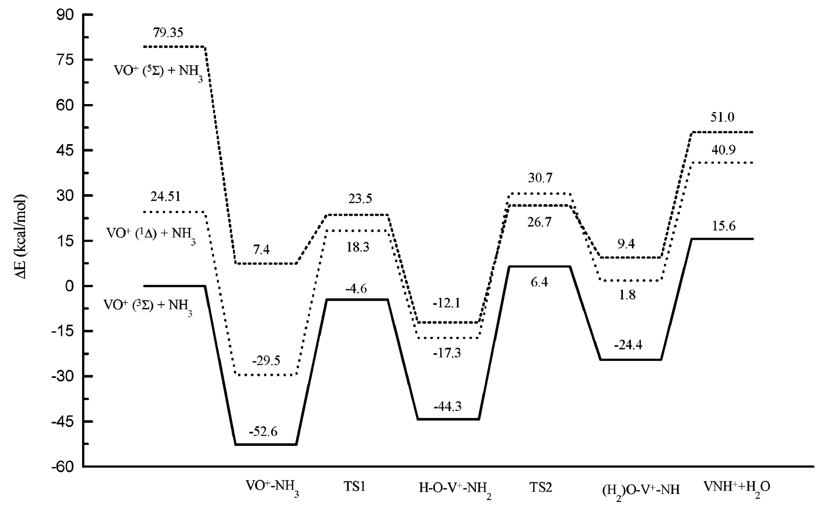

Figure 2. B3LYP/DZVP$_{opt}$ triplet, singlet and quintet potential energy surfaces for the reaction of VO^+ with NH_3. Energies are in kcal/mol and relative to the ground-state reactants.

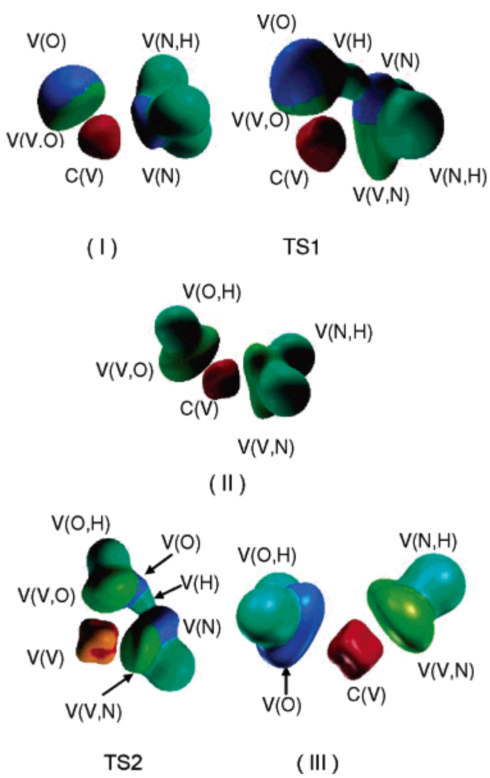

Figure 3. ELF localization domains for all the key minima involved in the singlet spin state VO^+ reaction path.

the N−H covalent bond is already broken whereas the O−H one is not yet formed. After this transition state, the V(O) and V(H) basins collapse as a consequence of a fold catastrophe, producing a disynaptic V(O,H) basin, characteristic of a covalent O−H bond. The formation of this intermediate provokes an important increase in V−O and V−N strength, as demonstrated by the increase of the corresponding basin population. Therefore, the hydrogen transfer involves two steps, in the first one the N−H bond is broken, whereas in the second one, the formation of a O−H covalent bond takes place.

Once again, the presence of the second transition state involves the formation of a monosynaptic V(H) basin populated by 0.38 electrons. The V(V,N) basin increases slightly its population, showing a more symmetrical charge distribution on the two V(V,N) basins. In the case of the V(V,O) basins, there is a loss of more than one electron. As can be seen in Table 1, this structure is characterized by the presence of a V(V) basin, which is populated by almost two electrons. As a consequence, the C(V) basin decreases remarkably its population, which now contains only 19.07 electrons. Within ELF analysis, the electron density arising from the metal d subshell belongs mainly to the metal core. Therefore, this depleted core basin population indicates that the small contribution of the metal to the different disynaptic basins, namely V(V,N) and V(V,O), has mainly d character. In the previous structures, the presence of almost 21 electrons in the core, which is the value expected for the s^1d^3 electronic configuration that characterizes the lowest energy triplet state of V^+ bare cation, indicates that the corresponding contribution of vanadium is mainly of s character. In going from this transition state to the second intermediate of the reaction, the population of this basin decreases even more to 18.35 electrons, but in this case, most of this charge transfer increases the population of one of the disynaptic V(V,N) basin. The presence of two monosynaptic V(O) basins accounting for the two oxygen lone pairs indicates that the structure is already topologically prepared for the loss of the H_2O molecule. The V−O bond is already absent in this intermediate (see Table 1). The V−N bond is strengthened as a consequence of the transfer of charge caused by the disappearance of the V(V,O) disynaptic basins, presenting an electron population that enables us to classify the bond between the vanadium and nitrogen atoms as a double bond.

After the loss of the H_2O molecule, the VNH^+ fragment suffers some redistributions of charge, as can be seen in Table 1. The C(V) population increases again, arriving to almost 21 electrons, at the expense of the V(V,N) basin population.

FeO^+ Insertion into N−H Bond. The geometrical parameters of stationary points for both the ground and first excited states are reported in Figure 4, and the potential

Table 1. Basin Population, $\bar{N}$, and Integrated Spin Densities, $\langle S_Z \rangle$, of the Key Minima and Transition States Found along the Reaction Path of VO^+ ($^3\Sigma$) and NH_3

	$VO^+(^3\Sigma)$		I		II		TS1		TS2		III		VNH^+	
basin	$\bar{N}$	$\langle S_Z \rangle$	$\bar{N}$	$\langle S_Z \rangle$	$\bar{N}$	$\langle S_Z \rangle$	$\bar{N}$	$\langle S_Z \rangle$	$\bar{N}$	$\langle S_Z \rangle$	$\bar{N}$	$\langle S_Z \rangle$	$\bar{N}$	$\langle S_Z \rangle$
C(V)	21.00	1.09	20.98	1.04	20.83	0.99	20.82	1.04	19.07	0.77	18.35	0.64	20.95	1.14
Vasym(V)									1.94	0.374	0.16	0.06		
V(O)	4.19	−0.05	3.84	−0.05	4.31	−0.04			1.53		2 × 2.11	0.01		
V(N)			2.04	0.03	1.50				2.22	−0.06				
V(N,H)			1.94		1.98		2.01	−0.01	2.06	−0.04	2.14	−0.04	2.06	−0.06
V(V,O)	2.68	−0.03	3.07	−0.02	2 × 1.27		5.62		2 × 2.06	2 × 0.01				
V(V,N)					2.06	0.03	1.52		1.35	−0.03	2.09	−0.04	4.58	−0.06
V(V,N)							1.88	−0.01	1.29	−0.02	2.01	−0.03		
V(H)					0.53				0.38	0.01				
V(O,H)							1.87		1.78		1.72			

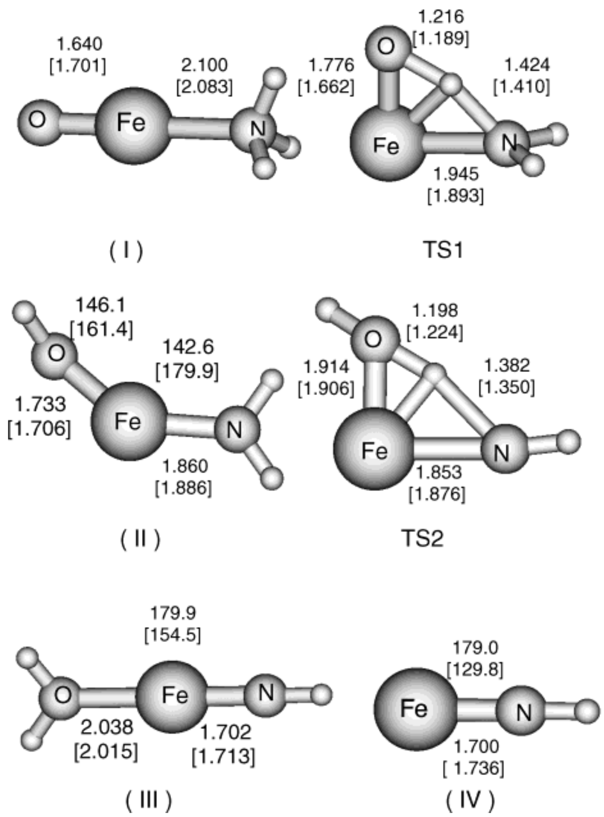

Figure 4. Geometric parameters of minima and transition states on the B3LYP/DZVP$_{opt}$ sextet and quartet potential energy surface for the reaction of FeO^+ with NH_3. Bond lengths are in angstroms and angles in degrees. Quartet spin parameters are reported in brackets.

energy surfaces for high- and low-spin states of the oxide cation calculated at the B3LYP/DZVP$_{opt}$ level are sketched in Figure 5.

The oxide cation possesses a sextet ground state separated by 7.9 kcal/mol from the first quartet excited state. This energy gap agrees with other theoretical values found in the literature,[61,62] being the range of the predicted values, however, quite large. The paths corresponding to both multiplicities have been investigated, and as clearly appears from Figure 4, they are very close in energy. As a consequence, the assignment of the ground state multiplicity of minima and transition states is questionable for the majority of them as well as the occurrence of surface spin crossings.

Our results again suggest that the mechanism of oxidative addition is operative to form the intermediate HO−Fe−NH_2^+. The first step of the reaction of FeO^+ with ammonia is the exothermic formation, along both high- and low-spin PES's, of the ion−molecule complex (I), whose ground state multiplicity is sextet. The next step of the reaction is the insertion of FeO^+ into the N−H bond of ammonia leading to the intermediate HO−Fe^+−NH_2 (II). A hydrogen atom is shifted from nitrogen to the oxygen atom through the TS1 transition state. We succeeded in locating the structures, which are four-center complexes, of the transition states related to this step for both the ground quartet state and the excited sextet one. Due to the change of the ground state spin multiplicity, a surface crossing is localized in this region of the PES, and it is noteworthy that along both the low- and high-spin surfaces the barrier heights are well below the reactants' limit. The spin multiplicity is conserved in the formation of the insertion intermediate, which seems to have a quartet multiplicity even if the difference in energy with respect to the sextet is very small.

The next step is the formation of the water complex (H_2O)Fe^+−NH (III) after overcoming an energy barrier corresponding to the TS2 four-center transition state. In going from intermediate II to intermediate III, we can predict the occurrence of another spin crossover from the quartet to the sextet surface between TS2 and III moieties, even if the difficulty in assigning the ground state spin multiplicity to the species in this region of the PES prevents us from establishing exactly where the spin inversion takes place. Although the energy needed to overcome the barrier for TS2 is quite large, it is noticeable that the barrier heights do not exceed the reactants' limit. From intermediate III, the formation of the dehydration products proceeds directly, without transition state and conserving the spin. The calculated energy of reaction is 6.9 kcal/mol and agrees very well with the exothermicity value of about 5 kcal/mol suggested experimentally.[30]

A simple breaking of the Fe−N bond can generate the other ionic products of the reaction directly from the insertion intermediate. This process, on the basis of our results, is predicted to be exothermic by 16.8 kcal/mol and, therefore, competitive with respect to dehydration products formation.

(60) Krokidis, X.; Goncalves, V.; Savin, A.; Silvi, B. *J. Phys. Chem. A* **1998**, *102,* 5065.
(61) Filatov, S.; Shaik, S. *J. Phys. Chem. A* **1998**, *102,* 3835.
(62) Fiedler, A.; Schröder, D.; Shaik, S.; Schwarz, H. *J. Am. Chem. Soc.* **1994**, *116,* 10734.

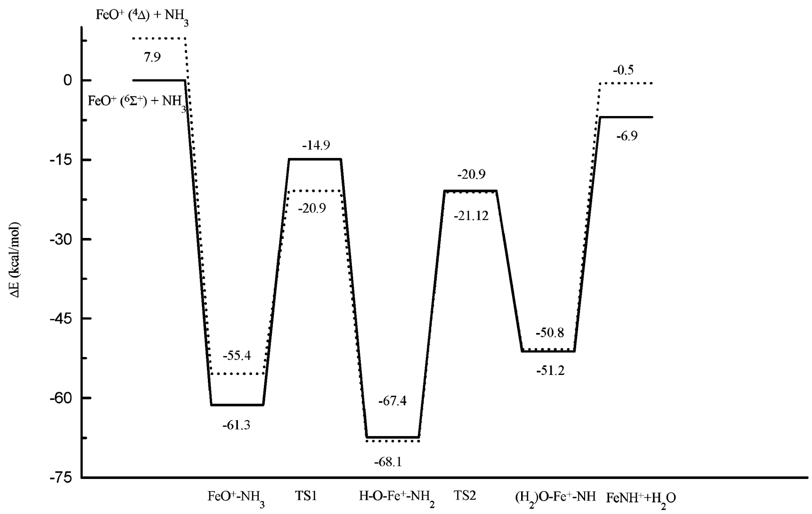

Figure 5. B3LYP/DZVP$_{opt}$ sextet and quartet potential energy surfaces for the reaction of FeO^+ with NH_3. Energies are in kcal/mol and relative to the ground-state reactants.

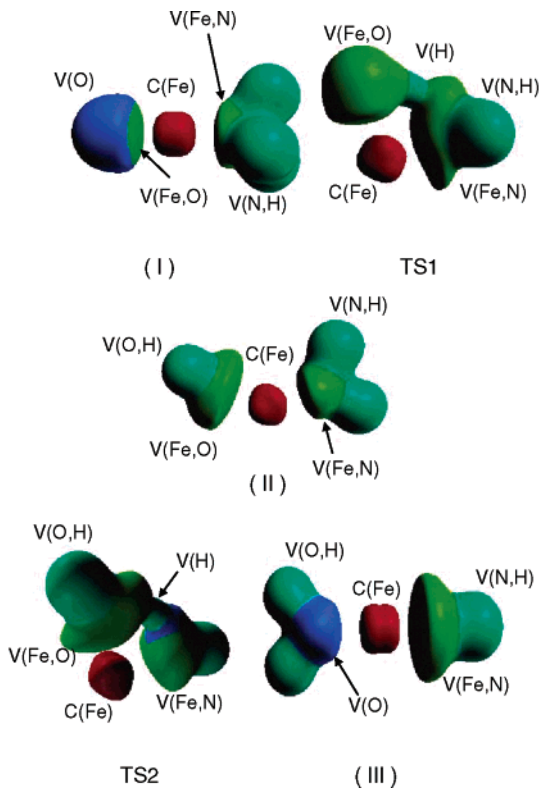

Figure 6. ELF localization domains for all the key minima involved in the sextet spin state FeO^+ reaction path.

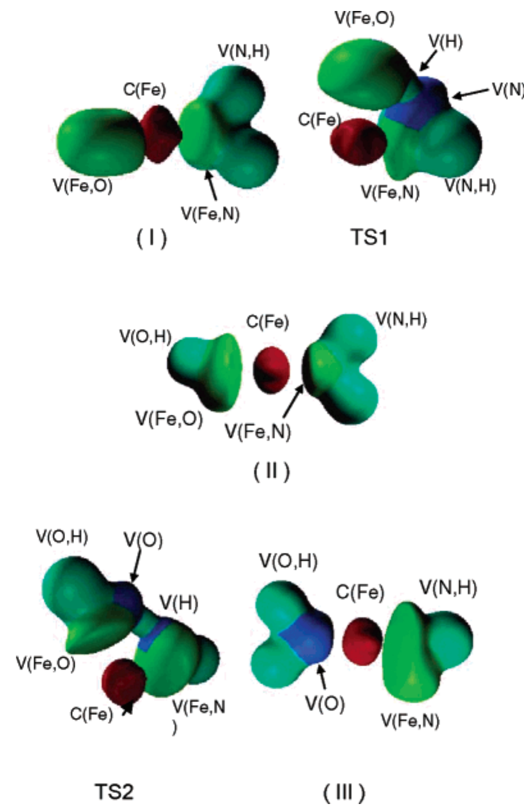

Figure 7. ELF localization domains for all the key minima involved in the quartet spin state FeO^+ reaction path.

As can be seen in the corresponding pathways (Figure 5), quartet and sextet spin states are very close in energy for almost all the species involved in the reaction. Therefore, we have performed the ELF analysis of all the involved minima and transition states for both quartet and sextet spin states. Figure 6 shows the localization domains corresponding to the sextet spin states, and Figure 7 shows the same species corresponding to the quartet one.

The population of valence and core basins that noticeably vary during the reaction are listed in Tables 2 and 3.

The first $FeO(NH_3)^+$ minimum in its sextet spin state is characterized by the presence of nine valence basins, five of which are disynaptic ones, namely V(Fe,N), V(Fe,O), and three V(N,H), which correspond to the Fe−N, Fe−O, and N−H covalent bonds, and have populations of 2.08, 2.48, and 1.94 electrons, respectively. The presence of a monosynaptic V(O) basin accounts for the existence of the oxygen lone pairs. The atomic contributions (in the sense of AIM) of iron and nitrogen to the disynaptic V(Fe,N) basin, for both spin state complexes, show that the Fe−N bond is mostly ionic, the Fe contribution being less than 5%. However, this basin can be considered as a disynaptic one. The analogue complex in its quartet spin state, which has been found around 6 kcal/mol above in energy, shows some topological differences with respect to the before-described sextet state.

Table 2. Basin Population, $\bar{N}$, and Integrated Spin Densities, $\langle S_Z \rangle$, of the Key Minima and Transition States Found along the Reaction Path of FeO^+ ($^6\Sigma$) and NH_3

	FeO^+ ($^6\Sigma$)		I		TS1		II		TS2		III		$FeNH^+$	
basin	$\bar{N}$	$\langle S_Z \rangle$	$\bar{N}$	$\langle S_Z \rangle$	$\bar{N}$	$\langle S_Z \rangle$	$\bar{N}$	$\langle S_Z \rangle$	$\bar{N}$	$\langle S_Z \rangle$	$\bar{N}$	$\langle S_Z \rangle$	$\bar{N}$	$\langle S_Z \rangle$
C(Fe)	24.07	1.80	23.78	1.85	23.81	1.90	23.71	1.88	23.93	1.85	23.84	1.75	23.94	1.75
Vasym(Fe)														
V(O)	4.70	0.51	4.58	0.43					1.49		2 × 2.24	0.01		
V(N)											0.35	0.04		
V(N,H)			1.94		1.98	0.02	2.10	0.07	2.11	0.10	2.21	0.13	2.38	0.17
V(Fe,N)			2.08	0.04	1.90	0.02	1.72	0.12	2.31	0.18	2.03	0.23	4.54	0.54
V(Fe,N)					1.74	0.08	1.53	0.11	2.46	0.24	2.44	0.29		
V(Fe,O)	2.09	0.15	2.48	0.15	5.37	0.36	5.80	0.19	2.17	0.04				
V(Fe,O)					1.52	0.07			2.15	0.04				
V(H)					0.43				0.35					
V(O,H)							1.79	0.03	1.76	0.01	1.70			

Table 3. Basin Population, $\bar{N}$N, and Integrated Spin Densities, $\langle S_Z \rangle$, of the Key Minima and Transition States Found along the Reaction Path of FeO^+ ($^4\Delta$) and NH_3

	FeO^+ ($^4\Delta$)		I		II		TS		TS2		III		$FeNH^+$	
basin	$\bar{N}$	$\langle S_Z \rangle$	$\bar{N}$	$\langle S_Z \rangle$	$\bar{N}$	$\langle S_Z \rangle$	$\bar{N}$	$\langle S_Z \rangle$	$\bar{N}$	$\langle S_Z \rangle$	$\bar{N}$	$\langle S_Z \rangle$	$\bar{N}$	$\langle S_Z \rangle$
C(Fe)	24.20	1.75	24.11	1.72	23.94	1.46	23.98	1.66	24.09	1.78	24.11	1.66	24.15	1.72
Vasym(Fe)													0.12	0.03
V(O)					1.50				1.45		2.24	0.01		
V(N)					1.87				2.18	−0.14				
V(N,H)			1.94		2.01		2.11	−0.07	2.08	−0.08			2.06	−0.06
V(Fe,N)			2.08	0.04	1.58	0.01	1.49	−0.06	2.45	−0.11	2.50	−0.08	2.79	−0.13
V(Fe,N)							1.48	−0.06			2.22	−0.05	1.77	−0.05
V(Fe,O)	3.19	−0.11	6.76	−0.24	2.64	0.02	2.54	0.05	2.19	0.02				
V(Fe,O)	3.49	−0.13			2.77	0.02	3.23	0.06	2.20	0.02	2.19	0.02		
V(H)					0.43	0.01			0.35					
V(O,H)							1.84	0.02	1.76	0.01	1.71			

In this case, no V(O) basin is present. There are, instead, two disynaptic V(Fe,O) basins, mainly formed from the oxygen contribution. At this point of the reaction, an intersystem crossing takes place, and as a consequence, the first transition state of the reaction, TS1, has a quartet spin state. This transition structure belongs to a different structural stability domain. Indeed, in going from the first minimun to TS1, a plyomorphic step, which increases the morphic number by one, takes place. In fact, as in the previously studied reaction, the proton migration produces a simultaneous transformation in which one of the V(N,H) disynaptic basins disappears, and at the same time, two monosynaptic basins, V(N) and V(H), arise. Chemically, the covalent N−H bond is broken giving rise to a nitrogen lone pair and a V(H) monosynaptic basin. In TS1, the V(N) basin is populated by 1.87 electrons whereas the V(H) one is populated by 0.43 electrons. Figure 6 clearly shows that in this intermediate structure the N−H bond is already broken, whereas the O−H one is not yet formed. Therefore, as in the vanadium oxide reaction, the proton transfer can be described as a two-step process: the first one involves the breaking of a covalent N−H bond and is followed by the formation of a O−H one. From the catastrophe theory viewpoint, the change of structural stability domain can be described as a bifurcation catastrophe of the fold type. At the same time, in going from the first minimum to the transition structure, an important redistribution of charge takes place (see Tables 2 and 3). The population of the V(O) basin, already present in the $FeO(NH_3)^+$ ground state complex, decreases markedly, being populated by only 1.50 electrons in the quartet TS1 state. As a consequence, a transfer of charge to the V(Fe,O) valence basin that increases its population in almost three electrons takes place. Conversely, the disynaptic V(Fe,N) basin suffer a loss of 0.5 electrons; i.e., it contains 1.58 electrons, which correspond to a weak single bond. The C(Fe) basin increases slightly its population from 23.78 in the first complex to 23.94 electrons in the TS1 quartet spin state. The iron core basin population continues to vary slightly during the evolution of the reaction being always quite close to 24.0 electrons, which corresponds to the expectation value for a ^{6}D (sd^6) state of Fe^+. This means that the contribution of charge coming from the metal in all the species present along the path has mainly an s-character.

As the reaction evolves toward the insertion intermediate (II), another important topological change takes place. Once again a fold bifurcation catastrophe occurs causing the change to the next structural stability domain. As a consequence, the two monosynaptic basins, V(O) and V(H), disappear, collapsing into a disynaptic V(O,H) basin, which can be ascribed to an O−H bond. At the same time, the other monosynaptic basin, V(N), also vanishes as a consequence of a cusp catastrophe (miomorphic process, $\Delta\mu < 0$). It must be noted the presence of two disynaptic V(Fe,N) basins, which indicates an increase of the Fe−N strength. The V(Fe,O) basin shows a slight increase in its population.

As can be seen from the corresponding pathway (see Figure 5), the sextet spin state structure is very close in energy (within 2 kcal/mol) to the ground state quartet state intermediate. From a topological point of view, both structures are quite similar (see Figure 6); i.e., they present the same number and type of basins. The basin populations show slight differences in going from the quartet to the sextet spin state.

The transfer of the second proton takes place by a similar mechanism; i.e., the formation of the transition structure involves the presence of a monosynaptic V(H) basin. Indeed, the TS2 quartet state, which shows a quite symmetrical structure (Figure 7), has similar topological characteristics to the already described TS1 structure. So, as in the case of the formation of the first transition state, a plyomorphic process takes place, and the bifurcation can be classified as a fold catastrophe. Simultaneously, a monosynaptic V(O) basin populated by 1.45 electrons appears. As a consequence of the formation of this basin, the population of the V(Fe,O) basin decreases in almost 1.40 electrons. The V(Fe,N) one suffers a loss of charge of about 0.50 electrons. Therefore, both Fe−O and Fe−N bonds are weakened by the formation of TS2. In this case, the monosynaptic V(H) basin has a population of 0.35 electrons, which indicates an increase of the ionicity of the interactions in comparison with the transfer of the first hydrogen. The other two monosynaptic basins, V(N) and V(O), are populated by 2.18 and 1.45 electrons, respectively.

The next step of the reaction involves a second intersystem crossing giving the $(H_2O)FeNH^+$ complex in a sextet ground spin state. Once again, the quartet state is quite close in energy (see Figure 5). As in the case of the formation of the first intermediate of the reaction, a miomorphic process causes the collapse of the two monosynaptic V(H) and V(O) basins, generating the second O−H bond. Simultaneously, the disynaptic V(Fe,O) basin disappears. Noticeable charge transfer between basins takes place. The V(N) basin shows an important loss of charge, from 2.18 electrons in the quartet TS2 to 0.35 in the second intermediate, whereas the V(Fe,N) one increases its population in almost two electrons. Two monosynaptic V(O) basins are already present in this intermediate structure, which means that the system is already structurally prepared for the detachment of the H_2O molecule.

After the loss of the water molecule, a further slight redistribution of charge takes place; i.e., the V(Fe,N) basin population is increased by 0.07 electrons whereas the V(N,H) basin gains 0.17 electrons.

4. Comparison between PES's

In this section we summarize and compare the behaviors along the paths for the insertion of vanadium and iron oxide cations into the N−H bond of ammonia both among them and with the reaction paths of the corresponding bare cations.[25,27]

In the past,[63−69] as a result of several studies on the reactivity of the early and late transition metal oxide cations, VO^+ has been found practically unreactive in contrast with FeO^+, which has been classified as very reactive and nonselective. This difference has been attributed to the strength of the M−O bond, which is quite strong in the case of vanadium but much weaker for iron. As a consequence, the oxygen ligand was postulated to greatly increase the reactivity of the iron ion being practically uninvolved in the chemistry of vanadium cation. Subsequently, several groups have developed a large body of work[62,70−72] around the reactivity of first-row transition metal oxides showing that the behavior of these systems is much more complicated than expected, and the results of the present study seem to confirm this viewpoint.

First of all, an insertion reaction would occur more efficiently for VO^+ because it conserves the spin compared to the occurrence of multiple surface crossings along the paths for the insertion of FeO^+.

The stabilization energy of the ion−dipole complex (I) is very high in both cases even if it is lower by about 10 kcal/mol for the vanadium oxide complex. This feature becomes more noticeable for the minima which follow along the paths. All the complexes lie lower in energy with respect to the dissociation limit, but those involving iron are considerably more stable than those involving vanadium, and the difference in the dissociation energy for FeO^+ and for VO^+ can be invoked to explain the difference in behavior. Analogously, the energy of ground TS1 and TS2 transition states is lower than the reactant asymptote of about 20 kcal/mol along the PES for the iron oxide, while for the vanadium oxide insertion only the first TS1 transition state is below the reactant asymptote. By looking at the barrier heights that are necessary to overcome to go from one minimum to another, however, it is noteworthy that they are all comparable among themselves.

The final dehydration products of the reaction are generated by direct breaking of the metal−oxygen bond and loss of a water molecule from the $(H_2O)M^+{-}NH$ complex. The low stability of the iron oxide molecule leads to an exothermic process at the exit channel of the reaction with respect to the endothermic one for vanadium.

The present results can be directly compared with previously calculated[25,27] reaction pathways for the insertion of the bare V^+ and Fe^+ cations into the N−H bond of ammonia. We can consider, first, the main differences in reactivity due to the presence of the oxygen ligand along the paths for vanadium. As already underlined, no spin crossing is observed during the reaction of oxide in contrast to the bare cation. The TS1 barrier height is below the reactant asymptote, and the insertion intermediate, $HO{-}M^+{-}NH_2$, is significantly more stable than the corresponding $H{-}M^+{-}NH_2$. Then, it seems that until the formation of intermediate (II) the reactivity is enhanced. On the contrary, although the

(63) Stevens, A. E.; Beauchamp, J. L.; Freiser, B. S. *J. Am. Chem. Soc.* **1979**, *101*, 6449.
(64) Jackson, T. C.; Jacobson, D. B.; Freiser, B. S. *J. Am. Chem. Soc.* **1984**, *106*, 1252.
(65) Jackson, T. C.; Carlin, T. J.; Freiser, B. S. *J. Am. Chem. Soc*. **1986**, *108*, 1120.
(66) Kang, H.; Beauchamp, J. L. *J. Am. Chem. Soc*. **1986**, *108*, 7502.
(67) Schröder, D.; Schwarz, H. *Angew. Chem., Int. Ed. Engl.* **1990**, *29*, 1433.
(68) Clemmer, D. E.; Dalleska, N. F.; Armentrout, P. B. *Chem. Phys. Lett.* **1992**, *190*, 259.
(69) Schröder, D.; Schwarz, H. *Angew. Chem., Int. Ed. Engl.* **1995**, *29*, 1973 and references therein.
(70) Clemmer, D. E.; Aristov, N.; Armentrout, P. B. *J. Phys. Chem.* **1993**, *97*, 544.
(71) Chen, Y. M.; Clemmer, D. E.; Armentrout, P. B. *J. Am. Chem. Soc.* **1994**, *116*, 7815.
(72) Schröder, D.; Fiedler, A.; Ryan, S.; Schwarz, H. *J. Phys. Chem. A* **1994**, *98*, 68.

TS2 energy barriers for the bare ion and the oxide exceed both the reactant limits, the barrier that is necessary to overcome to obtain the intermediate (III) is considerably higher for the oxide, and whereas the final elimination of H_2 is thermoneutral, the water loss is endothermic by about 15 kcal/mol.

The situation is more clear for iron oxide since it confirmed its ability to transfer oxygen and to activate bonds. At a first glance, it appears that, although inefficient spin crossings between sextet and quartet surfaces occur along both the ion and the oxide paths, the oxygen ligand favorably influences the reactivity of the iron cation. The most relevant changes concern the TS2 barrier height, which is well below the reactant asymptote, and the exothermicity of product formation. The topological bond evolution of the dehydrogenation of ammonia by Fe^{+} has been previously studied, and the comparison with the present results indicates that the presence of the monosynaptic V(O) basin, which accounts for the oxygen lone pair, in the cation plays a key role, allowing a different reaction mechanism. Indeed, in the case of the interaction with the bare cation, the mechanism of transfer of the two hydrogen atoms is quite different.[27] For the transfer of the first one, it has been found that the Fe−H disynaptic basin is already formed in the transition structure. The second transfer instead involves the formation of a trisynaptic V(Fe,H,H) basin. Conversely, in the present case, the presence of the oxygen atom, with its lone pairs, favors the formation of a monosynaptic V(H) basin, for both hydrogen shifts.

From a topological point of view, the whole reaction mechanism, for both studied metal oxides, can be described as two successive intramolecular proton transfers, both of them being a two-step process, i.e., a process that involves an intermediate state in which the hydrogen atom is detached. For both hydrogen transfers, this two-step process involves first a breaking of a N−H bond followed by the formation of a covalent O−H bond. As has been previously pointed out,[60] this type of mechanism can be considered as a covalent process. However, the V(H) basin population present in all the transition structures indicates that the mechanism is not fully covalent, being the ionicity of the interactions greater in the second hydrogen transfer, as testified by the lower V(H) basin population.

Conclusions

The reaction PES's for vanadium and iron oxide cations insertion into the N−H bond of ammonia have been computed and analyzed. Both high- and low-spin potential energy surfaces have been characterized in detail at the B3LYP level, and newly developed DZVP basis sets optimized ad hoc for the employed functional have been used for the metals. The obtained energy profiles are compared with those for the analogous reaction paths of the bare cations, with the purpose of finding evidence for differences in behavior induced by the presence of the oxygen ligand. Oxidative addition of NH_3 across the M−O bond to form the $HO-M^{+}-NH_2$ intermediate and reductive elimination of a water molecule is the most conceivable mechanism for the reaction. Our calculations show that FeO^{+} high- and low-spin potential energy surfaces have crossing points, in correspondence of which spin inversion takes place, whereas the spin is conserved during the whole reaction of VO^{+}. The oxygen ligand changes drastically the energy profile of the iron ion enhancing the reactivity, whereas the induced changes in the PES of vanadium cation concern mainly the first part of the reaction until the formation of the insertion product. The picture of the behaviors along the paths has been supported by a topological description, based on the gradient field analysis of the electron localization function (ELF), of all the key minima and transition states along the reaction pathways in order to characterize the bonding.

Acknowledgment. Financial support from the Università degli Studi della Calabria and MIUR is gratefully acknowledged.

IC0348650